

COMPARISON OF FINNED TUBE AND PLATE-FINNED HEAT EXCHANGERS IN WASTE HEAT RECOVERY

Summary

The use of waste heat recovery devices on mobile units (trucks and ships) is usually limited by the available space and the application of compact heat exchangers is recommended for such purposes. The performance of the heat exchanger is defined by the optimized Rankine cycle (to achieve maximum power) and it depends on the mass flow and temperature of the flue gases and selection of the working fluid in Rankine cycle. An example of selection of the preheater performance (in case of water as the working fluid) is considered here, wherein the several surface types of finned tube and plate-finned heat exchangers are used, for which there are measured data of the heat transfer coefficient and friction factor. Heat exchangers are sized according to the criteria of maximum allowed velocity of the flue gases and shapes of the heat exchanger frontal area. The sized heat exchangers were compared with respect to the heat transfer coefficient, the area of the heat exchanger surface on the finned side, the volume of the heat exchanger and the pressure drop on both sides. From the comparison of the best plate-finned and the best finned tube heat exchangers it is concluded that in the recommended range of flue gases velocity (from 4 m/s to 6 m/s) the pressure drop at the gas side are similar (in the plate-finned heat exchanger it is in the range from 53.5 to 112 Pa and in the finned tube exchanger from 53.8 to 142.8 Pa), while the plate-finned exchanger has more than 50% smaller heat transfer area, compared to the finned tube one.

Key words: Heat exchangers, Heat transfer, Minimization of heat exchanger volume, Pareto frontier

1. Introduction

Burning of fossil fuels releases flue gases which cause serious problems in the environment, such as air pollution, global warming, ozone layer depletion and acid rains. In the diesel engine exhaust gases there is a significant amount of energy that can be utilized and so fuel consumption and environmental pollution can be reduced. Organic Rankine cycle is considered as one of the best technologies for the recovery of waste heat from the exhaust gases of heavy duty truck diesel engines.

Design process of ORC system is comprised of heat source selection, candidate fluid selection and thermodynamic cycle optimization, [1]. Dolz et al. [2] presented a study on the

bottoming Rankine cycle configuration with all the heat sources which includes waste energy recovery in a binary cycle.

Many studies on waste heat recovery of the diesel engines published in recent years deal with the working fluid selection, [3], [4], wherein the most often selected fluids are ethanol, toluene and water. Invernizzi et al. [5] proposed titanium tetrachloride as a new potential working fluid. Some authors used experimental organic Rankine cycle set [6], [7] and thermal energy storage [8] to investigate the feasibility of waste-heat-recovery from a diesel engine. Authors established different optimization models of ORC systems. Hajabdollahi et al. [9] made an optimization of ORC for diesel waste recovery in which they maximized the thermal efficiency and minimized the total annual cost. Shu et al. [10] performed parameters optimization with six indicators, including thermal efficiency, exergy destruction factor, turbine size parameter, total exergy destruction rate, turbine volume flow ratio and net power output per unit mass flow rate of exhaust.

Most of the published studies are based on the thermodynamic approach, not considering the technical and operating characteristics of the system components such as expanders and heat exchangers. One of the few works that take into account the technical characteristics of the components of the ORC system is [11] where the optimal working fluid and operating conditions are selected considering technological constraints of the expander, the heat exchangers and the feed pump. In several studies an exhaust gas heat exchanger performances are taken into consideration. Katsanos et al. [12] applied the procedure for the assessment of the optimum Rankine cycle parameters at different operating conditions in which the heat transfer coefficient and the pressure drop at both sides of the heat exchanger were calculated. Mavridou et al. [13] performed the sizing of a heat exchanger for truck applications using five different configurations and compared the conventional and the latest heat transfer enhancement technologies.

The use of ORC installation on mobile units (trucks) is usually limited by available space and for a given heat duty the heat exchanger should be as small as possible in size and weight, at a reasonable high pressure drop. For such purposes the application of compact heat exchangers is recommended and their sizing is of crucial importance.

Performance of the heat exchanger is defined by the optimized Rankine cycle (to achieve maximum power) and it depends on the mass flow rate and temperature of the flue gases and selection of working fluid in Rankine cycle. An example of selection of the preheater performance (in case of water as the working fluid) is considered here, wherein the several surface types of the finned tube and plate-finned heat exchangers are used, for which measured data of the heat transfer coefficient and friction factor are taken from literature [14]. The aim of this study is to compare two types of surfaces in terms of: obtainable overall heat transfer coefficient with restriction in gas velocity, i.e. the required finned area and required volume. Also, the impact of the shape of the heat exchanger frontal area on the maximal linear dimension of the heat exchanger and pressure drops in gas and liquid streams is examined.

2. Mathematical model

In this study we consider two types of compact heat exchangers (HE): finned tube (as depicted in the left panels in Figure 1) and plate-finned (right panels in Figure 1). Here we use surface types of the finned tube and plate-finned heat exchangers, from the catalogue in the EES (Engineering Equation Solver) program, in which measured data of the Colburn and friction factor in a range of Reynolds number exist. Once the surface type is chosen, we know all the geometric parameters of one heat exchanger cell and the frontal area (the area for the gas flow) is $A_{fr} = L_1 L_3$, where the height L_3 is defined by

$$L_3 = \begin{cases} N_{\text{row}} \cdot s_v & \text{for finned tube HE} \\ N_p \cdot b_2 + (N_p + 1) \cdot (b_1 + 2 \cdot a) & \text{for plate finned HE} \end{cases} \quad (1)$$

and

$$L_2 = \begin{cases} N_{\text{col}} \cdot s_h & \text{for finned tube HE} \\ N_{\text{off}} \cdot l_s & \text{for plate finned HE} \end{cases} \quad (2)$$

where N_{col} and N_{row} is the number of tube columns and rows in the finned tube HE, respectively, N_p is the number of passages of the liquid stream and N_{off} is the number of strip fins in the plate-finned HE. In both HE, L_2 is the length for pressure drop in gas stream flow, while length responsible for the pressure drop in liquid stream flow is L_1 in the case of plate-finned HE, and $N_{\text{col}}L_1$ in the case of the finned tube HE. It is important to note that in the case of plate-finned HE the height b_2 of a channel for the liquid flow can be freely chosen, while the selection of inner tube diameter d_i in the case of finned tube HE is limited by the outer tube diameter d_o and (if one wants to use standard tubes) by few variants of the tube wall thickness (here, we assume $d_i = 0.7654d_o$).

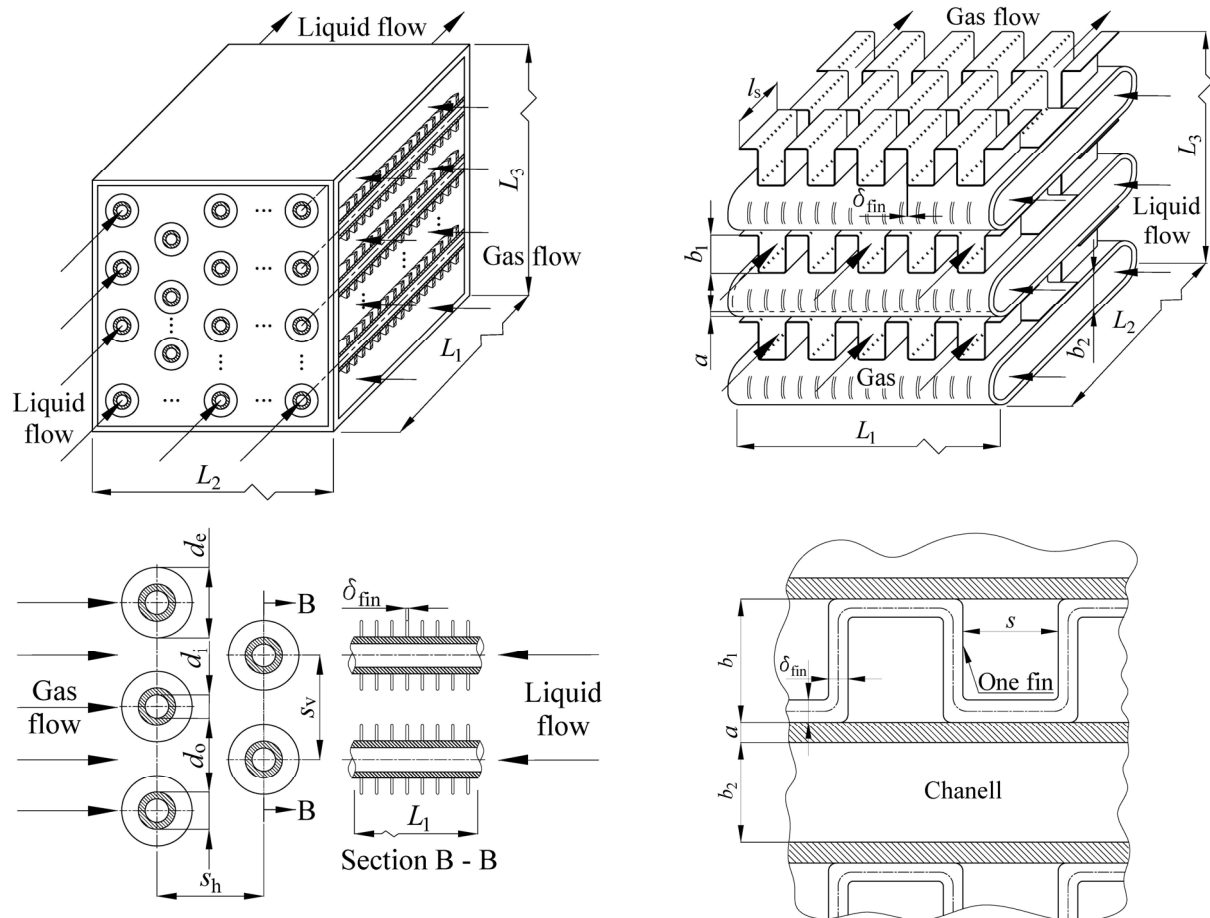


Fig. 1 Left panels: Finned tube heat exchanger and corresponding geometric parameters. 3D view of the heat exchanger with definition of lengths L_1 , L_2 , and L_3 (top) and a cross section view (bottom). Right panels: Plate-finned heat exchanger and corresponding geometric parameters. 3D view of the heat exchanger core with definition of lengths L_1 , L_2 , and L_3 (top) and a cross section view (bottom).

The problem is to size the heat exchanger when its heat duty \dot{q} , the heat capacity rate of hot and cold streams (\dot{C}_H and \dot{C}_C), the inlet temperatures ($T_{H,in}$ and $T_{C,in}$) and the outlet temperatures ($T_{H,out}$ and $T_{C,out}$) of both streams are known from the optimized Rankine cycle. The heat exchanger effectiveness is defined by

$$\varepsilon = \frac{\dot{q}}{\dot{C}_{\min}(T_{H,in} - T_{C,in})} \quad (3)$$

where \dot{C}_{\min} is the smaller value from \dot{C}_C and \dot{C}_H . In the Effectiveness- NTU method, the number of transfer units (NTU) is defined by

$$NTU = \frac{UA}{\dot{C}_{\min}} \quad (4)$$

where U is the overall heat transfer coefficient and A is the total gas side heat transfer area (finned area). Depending on the type of heat exchanger, there is a unique relationship between NTU and ε [15]. Here, we consider cross-flow gas-to-liquid heat exchangers with one stream unmixed, for which this relationship reads:

$$\varepsilon = \frac{1 - \exp\{C_R [\exp(-NTU) - 1]\}}{C_R} \quad (5)$$

where C_R is the heat capacity rate ratio $\dot{C}_{\min} / \dot{C}_{\max}$. If we neglect the thermal resistance in fins and tube/channel walls, the overall heat transfer coefficient is defined by

$$\frac{1}{U} = \frac{1}{\beta h_c} + \frac{1}{\eta_H h_H} \quad (6)$$

where h_c and h_H are the heat transfer coefficients on the cold (liquid) side and hot (gas) side, respectively; β is the ratio of the heat transfer surface area at the liquid side to the surface area at the gas side, and $\eta_H = 1 - (1 - \eta_{\text{fin}}) A_{\text{fin}} / A$ is the extended surface efficiency on the gas side, η_{fin} is the fin efficiency defined as

$$\eta_{\text{fin}} = \frac{\tanh(\Phi)}{\Phi}, \quad (7)$$

and A_{fin} is the fin surface area, and A is the total gas side heat transfer surface area.

Variable Φ in Equation (7) is defined as:

$$\Phi = \sqrt{\frac{2 \cdot h_o}{k \cdot \delta_{\text{fin}}}} \cdot L_c \cdot r^{0.13mL_c - 1.3863} \quad \text{for finned tube HE, and} \quad (8)$$

$$\Phi = (0.5 \cdot b_1 - \delta_{\text{fin}}) \cdot \sqrt{2 \cdot \frac{h_o}{k \cdot \delta_{\text{fin}}} \cdot \left(1 + \frac{\delta_{\text{fin}}}{l_s}\right)} \quad \text{for plate - finned HE.} \quad (9)$$

In above formulas k is material conductivity, $L_c = \frac{d_e - d_o + \delta_{\text{fin}}}{2}$ and $r = \frac{d_e}{d_o}$. Special case for finned tube HE is if $\Phi > 0.6 + 2.257 \cdot r^{-0.455}$ from Equation (8) then fin efficiency is defined as

$\eta_{\text{fin}} = a \cdot (m \cdot L_c)^{-b}$ and $a = r^{-0.246}$. Coefficient b depends on the diameter ratio r and is defined as if $r > 2$ then $b = 0.9706 + 0.17125 \cdot \ln(r)$, else if $r \leq 2$ coefficient b is $b = 0.9107 + 0.0893 \cdot r$. If $\Phi \leq 0.6 + 2.257 \cdot r^{-0.455}$ Equation (7) is valid.

It is known that the major part of thermal resistance is on the gas side, so it is necessary to focus on enlargement of h_H , which is defined by

$$h_H = j_H w_H \frac{\rho_H c_{p,H}}{Pr^{2/3}} \quad (10)$$

where j_H is the Colburn factor, ρ_H is the average gas density, w_H is the average gas velocity, $c_{p,H}$ is the gas average specific heat capacity at a constant pressure, and Pr is the Prandtl number.

In the same time, it is of great interest to reduce pressure drop in the gas stream, and this pressure drop is proportional to the friction factor f_H and to the w_H^2 . Both j_H and f_H decrease with increase of the Reynolds number ($Re = \rho_H w_H D_h / \mu_H$, D_h is the hydraulic diameter and μ_H is the gas viscosity). Thus, to obtain high h_H (high U and consequently small A) the small Re and high w_H are needed, while for small pressure drop the high Re and small w_H is required. Since these two sets of requirements are in contradiction, there is a need for optimization. The similar expressions are valid at the liquid-side of the heat exchanger, but it is important to note that the pressure drop in the liquid stream does not significantly influence the efficiency of the Rankine cycle. Thus, it is possible to keep the liquid stream velocity high, to obtain high h_C , regardless of the higher pressure drop in liquid stream. In that sense, the plate-finned HE could be better than finned tube HE since the liquid stream velocity can be adjusted arbitrarily by changing of b_2 value.

Described mathematical models have been implemented into EES software. The mathematical model of plate-finned heat exchanger contains 64 equations (some of them are specified in this paper and the rest of them are auxiliary equations from the EES routines for calculation of Colburn and friction factors and geometrical parameters of a given type of heat exchanger), while the model of tube-finned heat exchanger contains 63 equations. When the number of equations is equal to the number of unknowns the EES software is capable to solve the specified systems of equations regardless the order in which the equations are specified.

3. Results

We consider a preheater in the Rankine cycle with the following data: mass flow rate of flue gases $\dot{m}_H = 0.49$ kg/s in which the working fluid is water of mass flow rate $\dot{m}_C = 0.05093$ kg/s, the gas inlet and outlet temperatures are $T_{H,\text{in}} = 233.1^\circ\text{C}$ and $T_{H,\text{out}} = 159.5^\circ\text{C}$, the inlet and outlet temperatures of water are $T_{C,\text{in}} = 25.16^\circ\text{C}$ and $T_{C,\text{out}} = 192.5^\circ\text{C}$ (hot water) at pressure 1325 kPa. The exchanger heat duty is $\dot{q} = 36.27$ kW, at $\varepsilon = 0.8046$ and $NTU = 5$.

As it is explained above, the main interest here is to find HE with minimal surface area or volume, and for this a large h_H is required (i.e. small Re and high w_H). In most of the

existing HE the w_H is about 5 m/s and in some cases it is up to 10 m/s. Here, we will adopt the maximal allowable gas velocity $w_{Hmax} = 10$ m/s. Each surface type from the EES catalogue has defined the minimal Reynolds number (Re_{min}) at which the measured values of Colburn and friction factor are provided. The minimal value of the hydraulic diameter of the surface type is defined by Re_{min} and w_{Hmax} in the form

$$D_{hmin} = \frac{\mu_H Re_{min}}{\rho_H w_{Hmax}} \quad (11)$$

There are 3 of the finned tube surface types and 8 of the plate-finned surface types with the hydraulic diameter greater than D_{hmin} , and in the following we will show results for all three finned tube surface types and the best four plate-finned surface types listed in Table 1.

Table 1 Geometric characteristics of the considered finned tube and plate-finned surface types (α = heat transfer area/total volume; β = heat transfer area/volume between plates; δ_{fin} = fin thickness; N_f = number of fins per one meter; A_{fin} = fin surface area (including splitter); σ = free-flow area/frontal area)

Finned-tube surface type	Re_{min}	α	d_o	d_e	D_h	δ_{fin}	N_f	A_{fin}/A	σ	s_h	s_v	Mater. of fins
-	-	m^2/m^3	mm	mm	mm	mm	1/m	-	-	mm	mm	
fc_tubes_sCF-872c	400	446	10.67	21.62	4.425	0.48	343	0.876	0.494	20.32	24.77	Cu
fc_tubes_sCF-872	400	535	9.65	24.77	3.929	0.46	343	0.91	0.524	20.32	23.37	Al
fc_tubes_sCF-734	500	459	9.65	24.77	4.75	0.46	289	0.892	0.538	20.32	23.37	Al
Plate-finned surface type	Re_{min}	β	b_1	a	D_h	δ_{fin}	N_f	A_{fin}/A	σ	l_s	b_2	Mater. of fins
-	-	m^2/m^3	mm	mm	mm	mm	1/m	-	-	mm	mm	
sf_plate-fin_s12-1194D	200	1512	6.02	1	2.266	0.152	470	0.796	0.605	12.7	0.5	Al
sf_plate-fin_s16-1218D	200	1385	8.97	1	2.63	0.102	480	0.847	0.711	4.521	0.5	Al
sf_plate-fin_s18-1561	200	1548	6.35	1	2.38	0.102	651	0.923	0.660	3.175	0.5	Al
sf_plate-fin_s18-1612T	200	2133	7.98	1	1.567	0.152	635	0.882	0.636	3.175	0.5	Al

In the defined mathematical model it is possible to freely define three parameters in the case of plate-finned surface types and two parameters in the case of finned tube surface types (note that in the first case parameter b_2 can be freely chosen and in the second case d_i is uniquely related to d_o). For the first free parameter we selected the w_H , and at the first we kept it to its maximal value w_{Hmax} . For the second free parameter we used the ratio L_1/L_3 which defines the shape of the frontal area (square and different rectangles). We have analyzed five variants of this ratio: $L_1/L_3=1, 1.5, 1/1.5, 2$ and $1/2$. The third parameter in the case of plate-finned surface types could be either b_2 or the pressure drop at the liquid-side or the h_c . In the considered cases we used $b_2=0.5$ mm (to obtain high value of h_c at a reasonable high pressure drop at the liquid side). Figures 2 to 6 show obtained results (the finned area, overall heat transfer coefficient, heat transfer coefficients at the gas and liquid side, maximal and minimal dimensions among L_1, L_2 , and L_3 , number of rows/passages and number of columns/strip fins, and pressure drops at the gas and liquid side) for the seven heat exchanger surface types and the five different shapes of the frontal area.

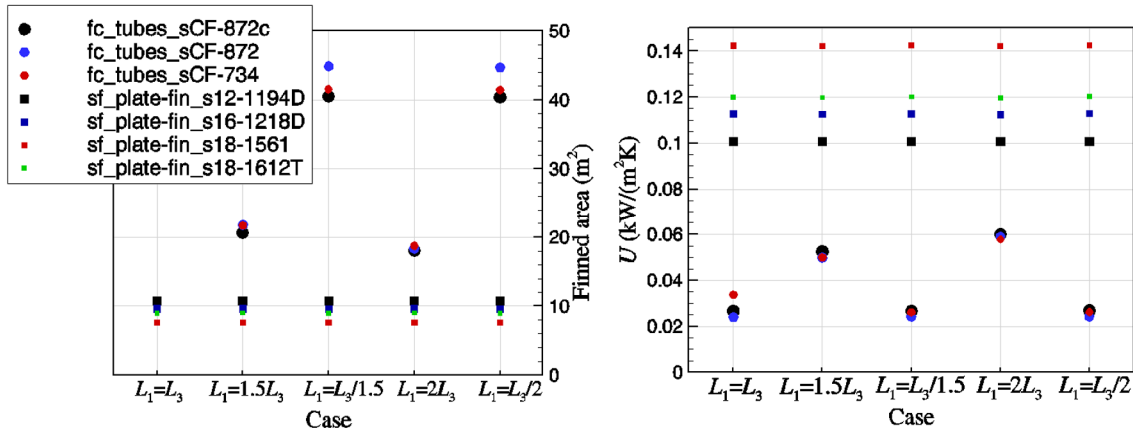


Fig. 2 Calculated finned area (left panel) and the overall heat transfer coefficient (right panel) for the seven surfaces and for five cases, for $w_H = 10$ m/s and $d_i = 0.7654 d_o$ or $b_2 = 0.5$ mm. The legend is the same for both panels.

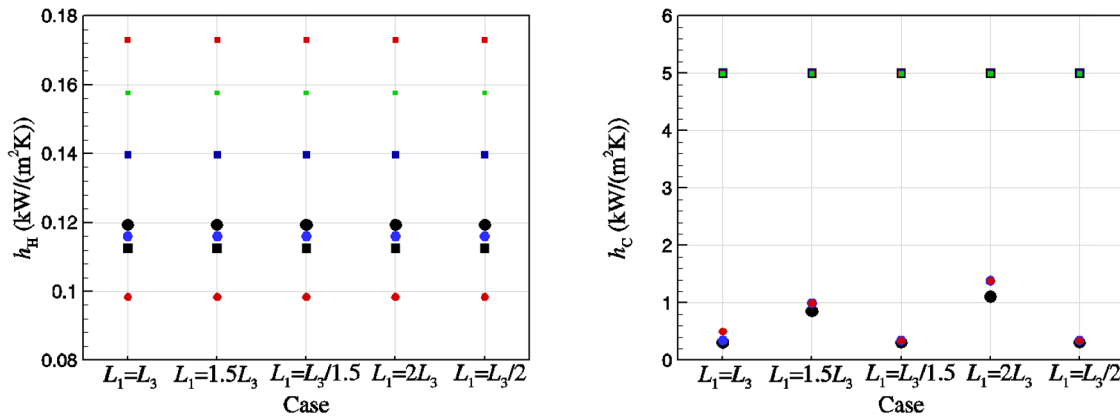


Fig. 3 Heat transfer coefficient at the gas side (left panel) and at the liquid side (right panel) for the seven surfaces and for five cases, for $w_H = 10$ m/s and $d_i = 0.7654 d_o$ or $b_2 = 0.5$ mm. The legend is the same as in Figure 2.

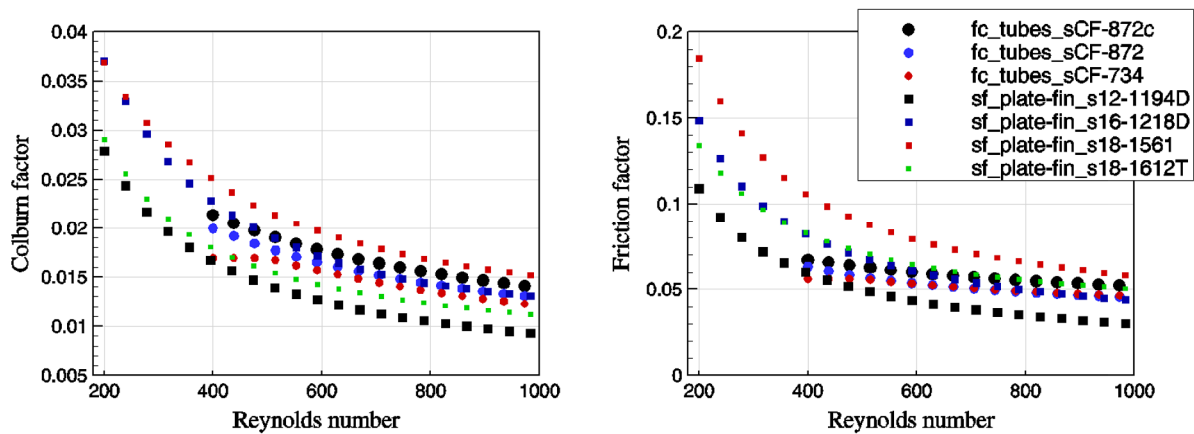


Fig. 4 Colburn and friction factor as a function of Reynolds number for the seven surfaces.

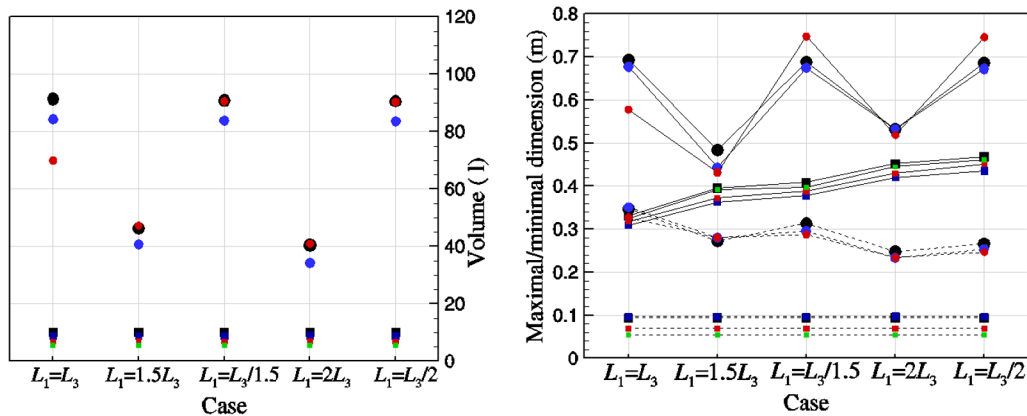


Fig. 5 Calculated heat exchanger volume (left panel) and the maximal and minimal linear dimension of heat exchanger (right panel) for the seven surfaces and for five cases, for $w_H = 10$ m/s and $d_i = 0.7654 d_o$ or $b_2 = 0.5$ mm. Dots in the right panel that define the maximal dimensions are connected by solid lines and dots denoting minimal dimensions by dashed lines. The legend is the same as in Figures 2 and 4.

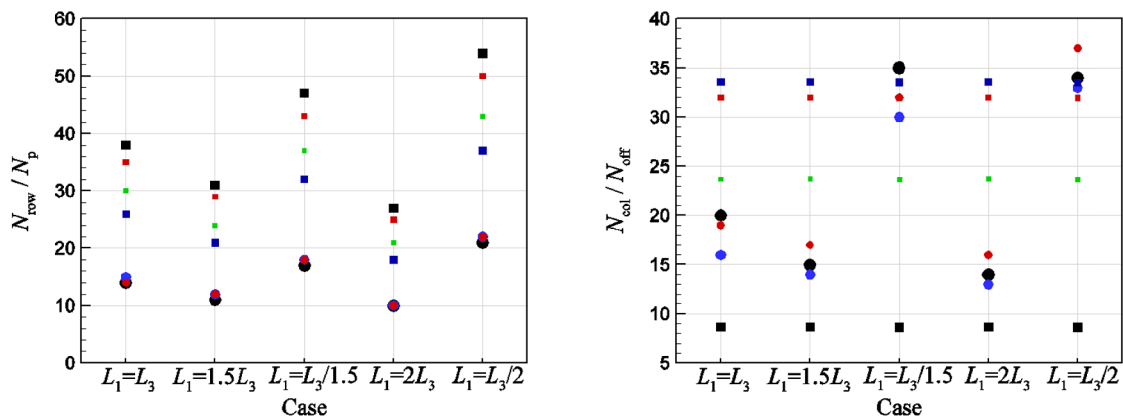


Fig. 6 Number of rows in finned tube heat exchanger or number of passages at liquid side in plate-finned heat exchanger (left panel) and number of columns in finned tube heat exchanger or number of strip fins in plate-finned heat exchanger (right panel) for the seven surfaces and for five cases, for $w_H = 10$ m/s and $d_i = 0.7654 d_o$ or $b_2 = 0.5$ mm. The legend is the same as in Figures 2 and 4.

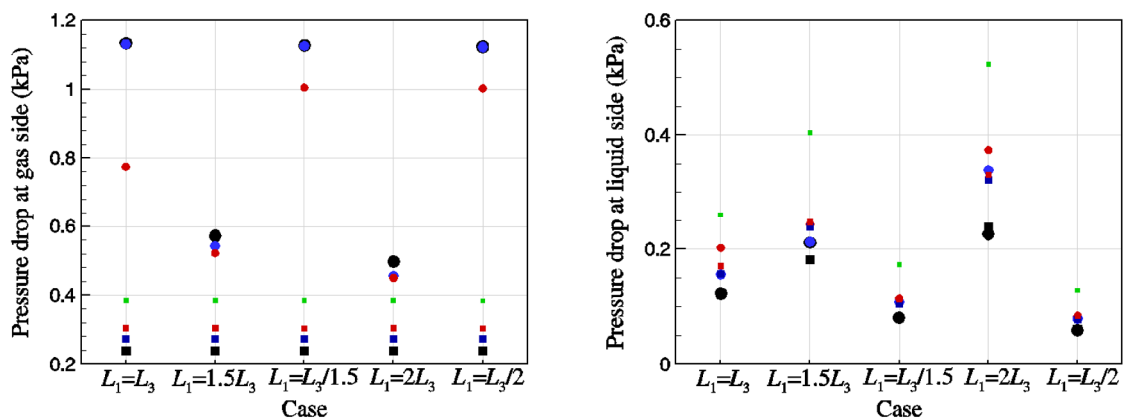


Fig. 7 Pressure drop in the heat exchanger at the gas side (left panel) and at the liquid side (right panel) for the seven surfaces and for five cases, for $w_H = 10$ m/s and $d_i = 0.7654 d_o$ or $b_2 = 0.5$ mm. The legend is the same as in Figures 2 and 4.

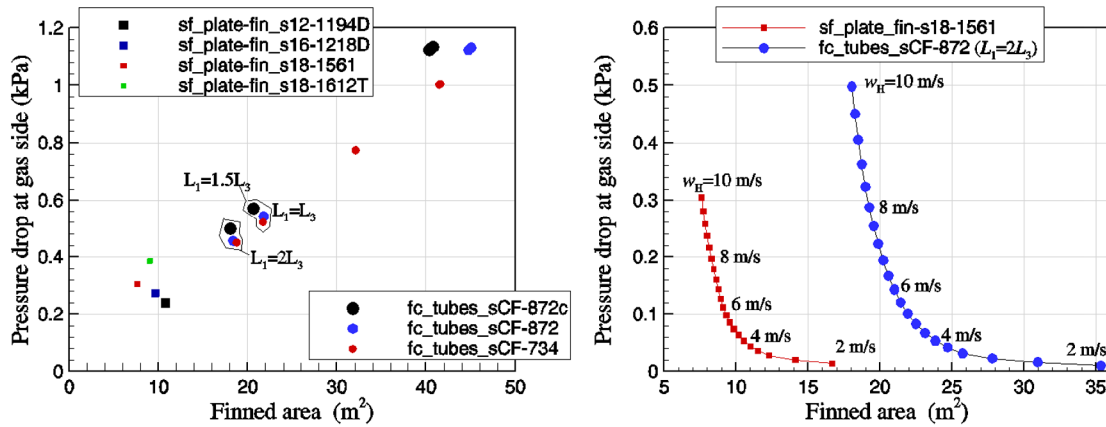


Fig. 8 Left panel: pressure drop in the heat exchanger at the gas side as a function of finned area (all points are calculated at gas velocity $w_H = 10$ m/s) for the seven surfaces and for five cases. Right panel: the same relationship as in the left panel for the best plate-finned surface and for the best finned tube surface, at different values of the gas velocity.

4. Discussion

It is visible in Fig. 2 that the use of plate-finned surface types results in smaller heat exchange area, due to higher overall heat transfer coefficients. All plate-finned surface types are better than the best finned tube surface types, and the smallest heat exchange area is obtained by using surface type sf_plate-fin_s18-1561. The overall heat transfer coefficient depends on heat transfer coefficient on both sides; see Equation (6), while the gas side is the critical one, since the heat transfer coefficient in gas is usually an order of magnitude smaller than in liquid. It is visible in Fig. 3 that plate-finned surfaces show higher heat transfer coefficient than finned tube surfaces at both gas and liquid sides. The higher h_H in plate-finned surface types can be explained by smaller Re_{min} and D_h (see Table 1) since for given w_H the smaller D_h results in smaller Reynolds number and higher Colburn factor (see Fig. 4), and consequently in higher h_H , see Equation (10). The higher h_C in plate-finned surface types can be explained by the fact that the Reynolds number in the liquid stream (and consequently h_C) in the case of plate-finned surface types can be kept sufficiently high, by free selection of parameter b_2 . In plate-finned surface types the overall heat transfer coefficient (and heat transfer area) does not depend on the shape of the frontal area (on the ratio L_1/L_3) and this is not the case in finned tube surface types. In case of finned tube surface types the Reynolds number in the liquid stream depends on the liquid mass flow through one tube (total liquid mass flow over the number of tube rows) and the inner tube diameter d_i which cannot be freely chosen. In the case of small liquid mass flow rate, the Reynolds number (and the value of h_C) can be increased by decreasing the number of rows. It is visible in left panel of Fig. 6 that in the case $L_1 = 2L_3$ (greater width and smaller height of the frontal area) the number of tube rows decreases, and consequently the Reynolds number, h_C (see right panel in Fig. 3), U (see right panel in Fig. 2), and pressure drop in liquid stream (see right panel in Fig. 7) increase, while A (left panel in Fig. 2) and number of columns decrease (see right panel in Fig. 6). The case $L_1 = L_3/2$ (smaller width and greater height of the frontal

area) has the opposite effect, and this option can be useful when the liquid mass flow rate and pressure drop in liquid stream are too high and the increased number of tube rows is required.

Fig. 5 shows that the volume of the plate-finned heat exchangers is significantly smaller than the volume of the finned tube heat exchangers. Also, in cases of plate-finned heat exchangers, the volume does not depend on the shape of the frontal area. In these heat exchangers, the minimal dimension is L_2 (in all cases it is smaller than L_1 and L_3), while the maximal dimension rises with deviation of L_1/L_3 from one (the maximal dimension is the smallest for $L_1/L_3=1$). In cases of finned tube heat exchangers, the shape of frontal area has a great impact on the volume and maximal dimension of heat exchanger. The volume is decreased by decreasing L_3 and increasing L_1 (that is why the number of rows is decreased, the Reynolds number in the liquid stream is increased and consequently h_c and U are increased, and A is decreased).

Fig. 7 shows pressure drops in gas and liquid streams, and it is visible that the pressure drop in gas stream (which should be kept very small) is smaller in the case of plate-finned surface types. This pressure drop is proportional to the friction factor, which is greater in plate-finned surface types (see right panel in Fig. 4), and length L_2 . In plate-finned heat exchangers L_2 corresponds to L_{\min} , and in finned tube heat exchangers to L_{\max} (compare L_{\min} and L_{\max} in the right panel of Fig. 5), and that is why the pressure drop is smaller in plate-finned heat exchangers. Similarly, in the liquid stream, the friction factor and velocity are greater in the case of plate-finned heat exchangers, but the length for the pressure drop is smaller (it is L_1 for plate-finned surface types and $N_{\text{col}}L_1$) therefore the pressure drop in liquid stream of plate-finned heat exchanger does not need to be greater than in finned tube heat exchangers.

For making the decision which variant of heat exchanger is the best in cases of restricted volume or maximal allowable dimension, it can be useful to see a diagram showing pressure drop in the gas stream (the most influential parameter on the efficiency of the Rankine process) as a function of the volume/maximal dimension or heat exchanger surface area. In such a diagram left panel in Fig. 8 shows all considered variants of heat exchanger, and in the right panel the Pareto frontier for the best one plate-finned and the best one finned tube surface type is shown. This frontier is obtained by varying the gas velocity w_H . At a smaller velocity the pressure drop is smaller, but the surface area is larger. The Pareto frontier contains solutions which show (when compared to other solutions) either a smaller pressure drop or surface area. From such diagram a designer can choose the best variant according to his preferences. The plate-finned heat exchanger is better choice since it requires smaller finned area, for the similar pressure drop at gas side. For $w_H=4$ m/s, the pressure drops in plate finned and finned tube heat exchangers are 53.5 and 53.8 Pa, respectively and corresponding finned surfaces are 10.55 and 23.85 m². At $w_H=6$ m/s the pressure drops are 111.9 and 142.8 Pa and required finned surfaces are 9.09 and 20.99 m².

5. Conclusion

The mathematical model for sizing of the plate-finned and finned tube heat exchangers, as well as the procedure for selecting the best variant of the heat exchanger is defined. The procedure is applied to a preheater with known heat duty and required efficiency. Seven surface types and five shapes of frontal area are analyzed and the best plate-finned and the finned tube heat exchangers are compared in terms of pressure drop at gas side and required finned area. In the recommended range of the flue gases velocity (from 4 m/s to 6 m/s) the pressure drop at the gas side are similar (in the plate-finned heat exchanger it is in the range from 53.5 to 112 Pa and in the finned tube exchanger from 53.8 to 142.8 Pa), while the plate-finned exchanger has more than 50 % smaller heat transfer area, compared to the finned tube one (at $w_H=4$ m/s, the finned area in the plate-finned and finned tube exchangers are 10.55 and 23.85 m², respectively, and at $w_H=6$ m/s these areas are 9.09 and 20.99 m²). This advantage can be explained by the fact that the Colburn factor (and the heat transfer coefficient) at the gas side is higher in the case of finned-plate heat exchanger than in finned tube surfaces. Also, the heat transfer coefficient at the liquid side is higher in the case of plate-finned surfaces, since the Reynolds number at liquid side can be freely adjusted by free selection of b_2 (which is not the case in finned tube surfaces, where the inner tube diameter is strictly related to outer diameter). In the case of plate-finned surface types the heat exchanger volume, its minimal dimension and overall heat transfer coefficient are not sensitive to the change of the shape of the heat exchanger frontal area, and this is additional advantage in the case of limited space for placement of heat exchanger.

REFERENCES

- [1] Amicabile, S., Lee, J. and Kum, D., A comprehensive design methodology of organic Rankine cycles for the waste heat recovery of automotive heavy-duty diesel engines, *Applied Thermal Engineering*, Vol. 87, pp. 574-585, 2015. <https://doi.org/10.1016/j.applthermaleng.2015.04.034>
- [2] Dolz, V., Novella, R., García, A. and Sánchez, J., HD Diesel engine equipped with a bottoming Rankine cycle as a waste heat recovery system. Part I: Study and analysis of the waste heat energy, *Applied Thermal Engineering*, Vol. 36, pp. 269-278, 2012. <https://doi.org/10.1016/j.applthermaleng.2011.10.025>
- [3] Panesar, A. S., Morgan, R. E., Miché, N. D. D. and Heikal, M. R., Working fluid selection for a subcritical bottoming cycle applied to a high exhaust gas recirculation engine, *Energy*, Vol. 60, pp. 388-400, 2013. <https://doi.org/10.1016/j.energy.2013.08.015>
- [4] Kölsch, B. and Radulovic, J., Utilisation of diesel engine waste heat by Organic Rankine Cycle, *Applied Thermal Engineering*, Vol. 78, pp. 437-448, 2015. <https://doi.org/10.1016/j.applthermaleng.2015.01.004>
- [5] Invernizzi, C. M., Iora, P., Bonalumi, D., Macchi, E., Roberto, R. and Caldera, M., Titanium tetrachloride as novel working fluid for high temperature Rankine Cycles: Thermodynamic analysis and experimental assessment of the thermal stability, *Applied Thermal Engineering*, Vol. 107, pp. 21-27, 2016. <https://doi.org/10.1016/j.applthermaleng.2016.06.136>
- [6] Yu, G., Gequn, S., Hua, Haiqiao, W. and Lina, L., Simulation and thermodynamic analysis of a bottoming Organic Rankine Cycle (ORC) of diesel engine (DE), *Energy*, Vol. 51, pp. 281-290, 2013. <https://doi.org/10.1016/j.energy.2012.10.054>
- [7] Zhang, Y., Xia, W. Y. G., Ma, C., Ji, W., Liu, S., Yang, K. and Yang, F., Development and experimental study on organic Rankine cycle system with single-screw expander for waste heat recovery from exhaust of diesel engine, *Energy*, vol. 77, pp. 499-508, 2014. <https://doi.org/10.1016/j.energy.2014.09.034>
- [8] Wilson, J. M. R., Singh, Abhishek K., Singh, Abhinav K., Ganapathy S.L.R., Waste heat recovery from diesel engine using custom designed heat exchanger and thermal storage system with nanoenhanced phase change material, *Thermal Science* 2017 Volume 21, Issue 1 Part B, pp. 715-727. <https://doi.org/10.2298/TSCI160426264W>

- [9] Hajabdollahi, Z., Hajabdollahi, F., Tehrani, M. and Hajabdollahi, H., Thermo-economic environmental optimization of Organic Rankine Cycle for diesel waste heat recovery, *Energy*, vol. 63, pp. 142-151, 2013. <https://doi.org/10.1016/j.energy.2013.10.046>
- [10] Shu, G., Li, X., Tian, H., Liang, X., Wei, H. and Wang, X., Alkanes as working fluids for high-temperature exhaust heat recovery of diesel engine using organic Rankine cycle, *Applied Energy*, Vol. 119, pp. 204-217, 2014. <https://doi.org/10.1016/j.apenergy.2013.12.056>
- [11] Maraver, D., Royo, J., Lemort, V. and Quoilin, S., Systematic optimization of subcritical and transcritical organic Rankine cycles (ORCs) constrained by technical parameters in multiple applications, *Applied Energy*, Vol. 117, pp. 11-29, 2014. <https://doi.org/10.1016/j.apenergy.2013.11.076>
- [12] Katsanos, C. O., Hountalas, D. T. and Pariotis, E. G., Thermodynamic analysis of a Rankine cycle applied on a diesel truck engine using steam and organic medium, *Energy Conversion and Management*, Vol. 60, pp. 68-76, 2012. <https://doi.org/10.1016/j.enconman.2011.12.026>
- [13] Mavridou, S., Mavropoulos, G. C., Bouris, D., Hountalas, D. T. and Bergeles, G., Comparative design study of a diesel exhaust gas heat exchanger for truck applications with conventional and state of the art heat transfer enhancements, *Applied Thermal Engineering*, Vol. 30, pp. 935-947, 2010. <https://doi.org/10.1016/j.applthermaleng.2010.01.003>
- [14] Kays, W. M. and London, A. L., *Compact Heat Exchanger - third edition*, Krieger Publishing Company, Florida, USA, 1991.
- [15] Shah, R. K. and Sekulić, D. P., *Fundamentals of heat exchanger design*, John Wiley & Sons, Inc., New Jersey, USA, 2003. <https://doi.org/10.1002/9780470172605>

Submitted: 09.5.2017

Accepted: 15.02.2018

Mario Holik, mag. ing. mech.
Prof. dr. sc. Marija Živić
Mechanical Engineering Faculty in
Slavonski Brod, J.J. Strossmayer University
of Osijek, Trg I. B. Mažuranić 2,
35000 Slavonski Brod, Croatia
Prof. dr. sc. Zdravko Virag
Faculty of Mechanical Engineering and
Naval Architecture, University of Zagreb,
I. Lučića 5, 10 000 Zagreb, Croatia
Antun Barac, mag. ing. mech.
Mechanical Engineering Faculty in
Slavonski Brod, J.J. Strossmayer University
of Osijek, Trg I. B. Mažuranić 2,
35000 Slavonski Brod, Croatia